A New Phenomenological-Based Rate-Dependent Hysteresis Operator for Hysteresis Characterization

Mohd Hanif Mohd Ramli,*
Faculty of Mechanical Engineering, Universiti Teknologi MARA, Malaysia

Mohd Azuwan Mat Dzahir
Department of Applied Mechanics and Design, Faculty of Mechanical Engineering, UTM, Skudai, Johor

**haniframli@salam.uitm.edu.my*

ABSTRACT

Hysteresis is a fundamental problem in most smart material based actuators. This phenomenon limits the performance of systems that driven by these actuators. Therefore, there is a need for a comprehensive and robust approach to model and control in order to eliminate the hysteresis effects. This paper presents an alternative modification to the original Bouc-Wen (BW) model so as to improve the characterization of smart actuators those are affected by hysteresis nonlinearity. For this purpose, an extended BW (EBW) model is proposed and formulated in the discrete-time domain. Due to nonlinear nature of the proposed model, an extended particle swarm optimization technique (EPSO) is used to properly validate EBW model. Through the simulation study, it is observed and confirmed that proposed model is capable of describing rate-dependent input-output relations, which is an important feature in the modeling of hysteresis phenomenon.

Keywords: *Modeling, Hysteresis, Smart Actuator, Particle Swarm Optimization, Bouc-Wen model.*

ISSN 1823- 5514, eISSN 2550-164X

Received for review: 2017-04-28
Accepted for publication: 2017-10-10
Published: 2018-04-15

Introduction

The study of hysteresis phenomenon has a long history. It is first observed in the field of ferromagnetism by James A. Ewing in 1881 [1]. This phenomenon is history dependent, i.e., it can be referred to a system that has memory, where the effects of input to the system are experienced with a certain delay in time. According to [2], hysteresis is a quasi-static phenomenon in which a sequence of periodic inputs produces a non-trivial input-output loop as the period of input increases without bound. This phenomenon arises in diverse fields ranging from physics to biology, from material science to mechanics, and from electronics to economics.

In recent decades, there has been a substantial advancement in various smart materials, which lead to a new class of sensing and actuation systems. A broad range of materials falls into this class, including piezoelectrics, magnetostrictives, shape memory alloys (SMA), electro-active polymers, and magnetorheological fluids. Their advantages include high flexibility in shape designs, versatility, and power–to–weight ratio compared to the traditional rigid actuators. In addition, their potential applications extend over a range of different industries including manufacturing [3]; for example, in semiconductor fabrication systems, robotics [4], automotive [5], medical applications [6], [7], also can be found in digital equipment such as in optical axis alignment of optical fiber, and positional control of charge coupled device (CCD) camera for enhancement of image resolution [8]. These materials however, are strongly exhibit hysteresis. As a result, systems that driven by these materials are directly affected by the hysteresis effects and give rise to poor performance [9], [10].

By and large, the common approach of characterizing the hysteresis behaviour is either by the law of physics or the phenomenological method [11]. A notable example of the physics-based model is Jiles-Atherton model, where it is the first model to describe the ferromagnetic hysteresis. Meanwhile, the phenomenological based models that have been exploited include:

1. Operator based models such as Preisach, Prandtl–Ishlinskii (P-I) operators, and their extensions which are normally based on the weighted superposition of many (and even infinitely many) fundamental hysteretic units known as hysteron,

2. Differential equation based (DEB) models, such as Coleman-Hodgdon model, Dahl model, and Bouc-Wen model.

It can be noticed that most of the existing models of hysteresis are initially developed to describe a particular type of hysteretic system but their mathematical forms are to a degree suitable for multi-disciplinary extensions. For example, Preisach model is initially developed to describe the dependence of magnetization on the magnetic field in ferromagnetic systems

in the mid-1930s. The model is widely used by the scientific community only after 50 years later following the works by [12]. Since then, the model has been extended to describe hysteresis phenomena in many other areas of science such as electromagnetism [13], economics, biology, geology, and has become one of the most utilized mathematical models in the literature [14]. Despite the fact operator based models demonstrate good capability to describe the hysteresis behaviour, they inherent relatively complex mathematical structures which require significant computation load during the control process, and thus limits their implementations in engineering fields [15]. Alternatively, differential equation-based models are also explored for modeling and control of smart actuators in the hope to simplify the mathematical structures. It is remarked that this class of operator can soundly describe a range of shapes of hysteretic effects, which match the behaviour of a wide class of hysteretic systems. In addition, it could provide physical insights to the problem, i.e., the changes to its parameters reflect the shape, amplitude, and orientation of the hysteresis curves. Recent results on the differential equations based models in the control and systems literature include [16]–[19].

In terms of hysteresis compensations, two main directions of control approaches are considered in order to mitigate the hysteresis nonlinearity and achieve closed loop system performance. The first approach is to employ the inversion of a hysteresis model or operator, which normally known as feedforward strategy. The second scheme is the typical feedback control methodology. Advanced control strategies such as adaptive control architecture and disturbance observer-based control have also been applied in order to better handle the compensation errors [15].

In the present paper, we aim to address the hysteresis characterization problem in smart material based actuators. An extended Bouc-Wen (EBW) model is introduced to solve and improve modeling of smart actuators those affected by hysteretic effects. Discrete-time domain is chosen for the modeling platform in order to simplify and facilitate model implementation. Three types of smart actuators, namely, a piezoelectric actuator (PEA), a giant-magnetostrictive actuator (GMA), and an ionic polymer metal composites actuator (IPMC) are used to verify modeling capacity of EBW. In this regard, an extended particle swarm optimization technique is exploited to appropriately validate the proposed EBW model.

Modeling Rate-Dependent Hysteresis Behaviour

Bouc-Wen model has received an increasing interest due to its capability to capture a range of shapes of hysteretic effects which match the behaviour of a wide class of hysteretic systems such as smart actuators, magnetorheological dampers, as well as mechanical isolation systems [9]. The general expression of BW model is given as [20]

$$y(t) = \rho k u(t) + (1-\rho) k x(t) \tag{1}$$

$$\dot{x}(t) = \xi \dot{u}(t) - \varphi |\dot{u}(t)| |x(t)|^{n-1} x(t) - \gamma \dot{u}(t) |x(t)|^{n} \tag{2}$$

where $y(t)$ denotes the output of the BW model; $u(t)$ and $x(t)$ represent the applied input and hysteresis state respectively; $0 < \rho < 1$ is the weighting constant; k is the stiffness coefficient; and ξ, φ, γ and $n \geq 1$ are the parameters which govern the shape and amplitude of the hysteresis curve.
Alternatively, the BW model (1)-(2) can be described as follows

$$\dot{y}(t) = (\rho k + k(1-\rho) z(t)) \dot{u}(t) \tag{3}$$

$$z(t) = \xi - \varphi \operatorname{sgn}(\dot{u}) \left| \frac{y(t) - \rho k u(t)}{k(1-\rho)} \right|^{n-1} \left(\frac{y(t) - \rho k u(t)}{k(1-\rho)} \right) - \gamma \left| \frac{y(t) - \rho k u(t)}{k(1-\rho)} \right|^{n} \tag{4}$$

For simplicity, consider $\rho = 0$, $k = 1$, and $n = 1$. Thus, Eqn. (3)-(4) can be expressed as

$$\dot{y}(t) = \xi \dot{u}(t) - \varphi |\dot{u}(t)| y(t) - \gamma \dot{u}(t) |y(t)| \tag{5}$$

Eqn. (5) is known as special case of BW model. From the literature, it is well known that BW model is rate-independent, i.e., limited to describing invariant hysteresis curves regardless the increment/decrement of the input frequency. This behaviour can be clearly seen in Figure 1(a). Besides, hysteretic effects found in most smart materials, especially in ferromagnetic and ferroelectric materials are rate-dependent e.g. as shown in Figure 1(b). In such cases, the use of standard BW model could yield considerable errors under inputs that are applied at varying rates. To cope with this problem, an extended version of BW model is developed based on Eqn. (5), which is discussed in the following subsection.

Discretization Procedure

In this study, discrete-time environment is chosen for development of the proposed rate-dependent hysteresis model. This consideration is taken to avoid numerical approximation, which normally degrades the system performance. Moreover, most of the equipment and experimental test rigs use digital environment.

In view of relation (5), its discrete version can be easily derived using Taylor Series Expansion method. Consider the following simple approximation of a first order derivative

$$y(t+\Delta t) = y(t) + \dot{y}(t)\cdot\Delta t + \ddot{y}(\varsigma)\cdot\frac{\Delta t^2}{2} \tag{6}$$

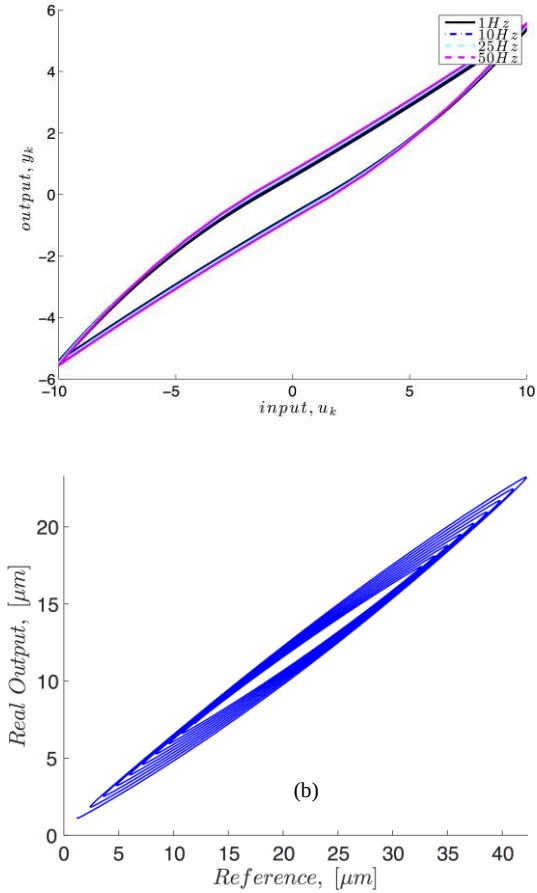

Figure 1: (a) Comparison of input-output relations described by relation (5) at difference frequencies. (b) Input-output relations measured in one of the commercial piezoelectric actuators.

where $\varsigma \in (t, t+\Delta t)$; Δt is the sampling period; $t = k\Delta t$ is the sampling instant. If $y(t) \neq 0$ and upon a simple rearrangement, the following relation is obtained

$$\dot{y}(t) = \frac{y(t+\Delta t) - (1-\eta_1)y(t)}{\Delta t} \tag{7}$$

in which $\eta_1 = \frac{\ddot{y}(\varsigma)}{y(t)} \cdot \frac{\Delta t^2}{2}$ is defined as a higher order positive function of Δt. If the sampling period Δt is chosen to be very small, then $(1-\eta_1)$ will be nearly equal to *1*. Thus, the derivative $\dot{y}(t)$ can be approximately expressed as

$$\dot{y}(t) \cong \frac{y(t+\Delta t) - \delta_1 y(t)}{\Delta t} \tag{8}$$

where δ_1 is a parameter which is nearly equal to *1* when Δt is sufficiently small. It can be easily seen that (8) is also valid even if $y(t) = 0$.

Similarly, $\dot{u}(t)$ can also be approximately expressed as

$$\dot{u}(t) \cong \frac{u(t+\Delta t) - \delta_2 u(t)}{\Delta t} \tag{9}$$

where δ_2 is a parameter which is nearly equal to *1* when Δt is sufficiently small.

In virtue of (8) – (9), and upon denoting $k\Delta t$ as k, Eqn. (5) can be expressed as

$$y_k = \delta_1 y_{k-1} + (\zeta - \psi \operatorname{sgn}(v_k) y_{k-1} - \alpha |y_{k-1}|) v_k \tag{10}$$

where v_k, ζ, ψ, and α are defined as

$$v_k = \frac{u_k - u_{k-1}}{\Delta t},\ \zeta = \xi \Delta t,\ \psi = \varphi \Delta t,\ \alpha = \gamma \Delta t \tag{11}$$

In order to insert a rate-dependent property and improve characterization accuracy, an absolute input difference term $\vartheta_k = \left|(u_k - u_{k-1})^r\right|$ is introduced into Eqn. (10). In this regard, r specifies the order of the difference term ϑ_k.

As a result, relation (10) becomes

$$y_k = \delta_1 y_{k-1} + \zeta(1 + \zeta_2 \vartheta_k - (\psi_1 + \psi_2 \vartheta_k) \operatorname{sgn}(v_k) y_k - (\alpha_1 + \alpha_2 \vartheta_k) |y_k|) v_k \tag{12}$$

Eqn. (12) will be known as extended-Bouc-Wen (EBW) model. Example of input-output relations generated by model (12) is given in Figure 2.

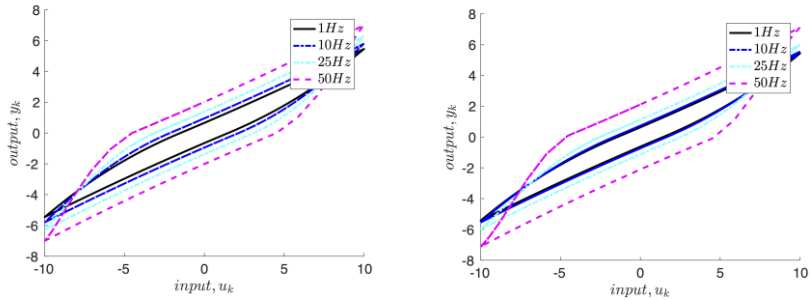

(a) (b)

Figure 2: Input-output curves described by Eqn. (12) at different frequencies with (a) $r = 1$, (b) $r = 2$.

Simulation results depicted in Figure 2 are based on sinusoidal input of $u_k = 10\sin(Hz * k * 0.0005)$. In this case, four different frequencies, namely 1 Hz, 10 Hz, 25 Hz, and 50 Hz are studied. The parameters of EBW model are chosen as; $\zeta_1 = 0.4346$, $\psi_1 = 0.0345$, $\alpha_1 = -0.05$, $\zeta_2 = 1e-6$, $\psi_2 = 0.09$, $\alpha_2 = -0.09$, and $\delta_1 = \delta_2 = 0.9995$. It can be witnessed that the curves generated by EBW model are varying with frequency changes, in other terms; the proposed model is a dynamic or rate-dependent hysteresis operator.

Model Validation

Experimental Environment

Figure 3 depicts the setup of experimental platform used in this section. Each smart actuator is driven by an analog input signal from the PC-based real-time controller. An analog interface board (AIO-163202F-PE) is used for data collection throughout the experimentation. The interface board is equipped with 32 analog inputs (AIs) and 2 analog outputs (AOs) with 16bits resolution and 500kHz sampling rate. The control algorithm is implemented on a personal computer (PC) by C language. The sampling frequency is set as 2kHz.

Experimental Results

To assess and verify the capacity of the proposed model, an extended particle swarm optimization (EPSO) technique is adopted where its velocity and position updates are given as

$$v_{k+1}^{i,d} = I_w \cdot v_k^{i,d} + \rho_1 \cdot r_1 \cdot (Pb_k^{i,d} - x_k^{i,d}) + \kappa_k \cdot \rho_2 \cdot r_2 \cdot (Gb_k^{i,d} - x_k^{i,d}) \qquad (13)$$

$$x_{k+1}^{i,d} = x_k^{i,d} + \kappa_k \cdot v_{k+1}^{i,d} \tag{14}$$

with κ_k is defined as

$$\kappa_k = \sigma \cdot \kappa_{k-1}(1 - \kappa_{k-1}) \tag{15}$$

where I_w is inertia weight; ρ_1 is cognitive learning gain; ρ_2 is social learning gain; r_1 and r_2 are random numbers, uniformly distributed in the range of [0,1]; $Pb_k^{i,d}$ is the best known position along the dth dimension of particle i in iteration k; $Gb_k^{i,d}$ is the global best known position among all particles along the dth dimension in iteration k; and $k = 1,2\ ;\ \ ;N$; denotes the iteration number, N is the maximum allowable iteration number, and σ is a positive constant.

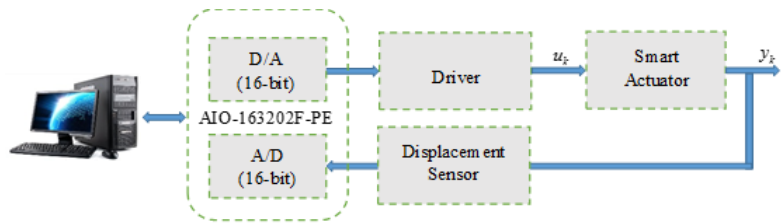

Figure 3: The diagram of experimental environment for model validation process.

Experimental data from the three aforementioned smart actuators are used for estimating parameters of EBW model using EPSO technique. For this purpose, the cost function is described by the root mean-square error (RMSE) as in Eqn. (16)

$$J_{RMSE} = \sqrt{\frac{\sum_{n=1}^{L}(Y_{\exp}^{n} - Y_{EBW}^{n})^2}{L}} \tag{16}$$

where $Y_{\exp}^{n}$ is the measured experiment data at the nth sampling instant, Y_{EBW}^{n} is the corresponding estimated output from the EBW model, and L is the total number of samples. Optimal parameter values are obtained when the following relation (17) is satisfied.

$$f(\zeta_1, \zeta_2, \psi_1, \psi_2, \alpha_1, \alpha_2) = \min(J_{RMSE}) \tag{17}$$

In the validation process, the parameters of EPSO algorithm are chosen as $r_1 = 1.5$, $r_2 = 2.5$, and $\sigma_1 = 4.0$. In addition, the population size N_s is set as 40 particles and κ_k is initiated by a random number.

Figure 4 illustrates and compares measured and estimated hysteresis curves with $r = 1$. Experimental studies related to both PEA and GMA use similar input excitations. Meanwhile, experiments done on IPMC considered much lower inputs to avoid curves reversal due to high hysteretic nonlinear property in this kind of smart actuator. Table 1 and Table 2 show the estimated value of each parameter of EBW model and the corresponding modeling accuracies in terms of numerical results. As can be clearly observed in Figure 4 and Table 2, good agreements are achieved between the simulated and measured input-output relations in the respective actuator.

Table 1: The optimal value of each parameter of EBW model pertaining to each smart actuator.

Parameter	IPMC	PEA	GMA
ζ_1	0.1584	0.3760	1.4666e-5
ζ_2	0.1745	0.016	0.9624
ψ_1	1.6875e-5	0.0099	6.737e-5
ψ_2	0.1483	0.0395	2.3021e-5
α_1	0.0945	-9.3084e-4	0.0292
α_2	0.7447	-8.7295e-4	9.4695e-5

Table 2: The RMSE value related to the measured and estimated hysteresis curves.

Type of actuator	Accuracy (RMSE) (μm)
IPMC	**0.0271** (0.05Hz of Input Frequency) **0.0795** (0.2Hz of Input Frequency)
PEA	**0.0248** (1Hz of Input Frequency) **0.0273** (10Hz of Input Frequency)
GMA	**0.1090** (1Hz of Input Frequency) **0.1056** (10Hz of Input Frequency)

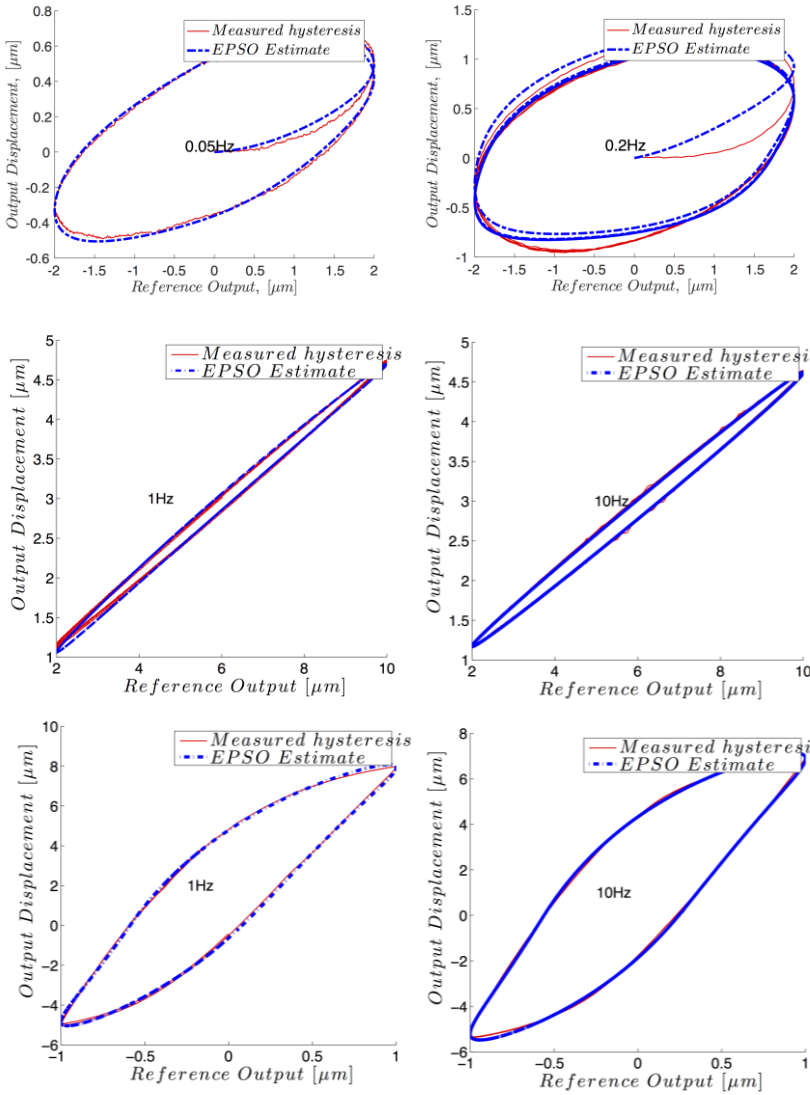

Figure 4: Comparison of input-output map between experimental data of (**Top**) IPMC, (**Centre**) PEA, (**Bottom**) GMA and EBW model at 0.05Hz to 10Hz.

Summary

In this paper, an alternative model modification is proposed to solve rate-independent property of the original BW model. In this case, the special case of BW model is used as the basis for developing the modified one and its establishment is realized in the discrete-time domain. This consideration is taken to avoid numerical approximation, which normally degrades the system performance. Moreover, most of the equipment and experimental test rigs use digital environment. From numerical simulation results, it is observed that the proposed model is capable of describing rate-dependent input-output relations. Thus, EBW model can be classified as a dynamic hysteresis model. Then, model validation process is carried out to verify the capacity of EBW model in terms of modeling and characterization of hysteretic smart actuators. The results show that estimated outputs of EBW model are well matched with the measured outputs obtained from IPMC, PEA, and GMA. This confirms that EBW model is not unique and shall be capable of fitting and matching the input-output relations of other smart actuators.

References

[1] R. V Iyer and X. Tan, "Control of hysteretic systems through inverse compensation," *IEEE Control Systems*, vol. 29, no. 1. pp. 83–99, 2009.

[2] J. H. Oh and D. S. Bernstein, "Semilinear Duhem model for rate-independent and rate-dependent hysteresis," *IEEE Trans. Automat. Contr.*, vol. 50, no. 5, pp. 631–645, 2005.

[3] Z. Wang, A. Witthauer, Q. Zou, G. Y. Kim, and L. Faidley, "Control of a magnetostrictive-actuator-based micromachining system for optimal high-speed microforming process," *IEEE/ASME Trans. Mechatronics*, vol. 20, no. 3, pp. 1046–1055, 2015.

[4] M. Karpelson, G. Y. Wei, and R. J. Wood, "Driving high voltage piezoelectric actuators in microrobotic applications," vol. 176, pp. 78–89, 2012.

[5] J. Melbert, C. Raupach, Q. Wang, and F. Niestroj, "Piezo actuators for automotive injection systems," *MTZ Worldw.*, vol. 67, no. 3, pp. 16–18, 2006.

[6] D. S. Levi, N. Kusnezov, and G. P. Carman, "Smart materials applications for pediatric cardiovascular devices," *Pediatr. Res.*, vol. 63, no. 5, pp. 552–558, 2008.

[7] E. Kaplanoglu, "Design of shape memory alloy-based and tendon-driven actuated fingers towards a hybrid anthropomorphic prosthetic hand," *Int. J. Adv. Robot. Syst.*, vol. 9, pp. 1–6, 2012.

[8] H.-P. Ko, H. Jeong, and B. Koc, "Piezoelectric actuator for mobile auto focus camera applications," *J. Electroceramics*, vol. 23, no. 2, p. 530,

2008.

[9] G. Y. Gu, L. M. Zhu, C. Y. Su, H. Ding, and S. Fatikow, "Modeling and Control of Piezo-Actuated Nanopositioning Stages: A Survey," *IEEE Transactions on Automation Science and Engineering*, vol. 13, no. 1. pp. 313–332, 2016.

[10] L. Zhang, Y. Xia, K. Lu, Y. Fang, Q. Lu, J. Ma, H. Pan, and D. Wang, "Motor-Driven Giant Magnetostrictive Actuator," *IEEE Trans. Magn.*, vol. 51, no. 10, 2015.

[11] Q. Xu and K. Kiong, *Advanced Control of Piezoelectric Micro-/NanoPositioning Systems*. New York, NY, USA: Springer US, 2016.

[12] A. A. Adly, I. D. Mayergoyz, and A. Bergqvist, "Preisach modeling of magnetostrictive hysteresis," *J. Appl. Phys.*, vol. 69, no. 8, pp. 5777–5779, 1991.

[13] X. Tan and J. S. Baras, "Modeling and control of hysteresis in magnetostrictive actuators," *Automatica*, vol. 40, no. 9, pp. 1469–1480, Sep. 2004.

[14] M. Dimian and P. Andrei, "Noise induced resonance phenomena in stochastically driven hysteretic systems," in *Journal of Applied Physics*, 2011, vol. 109, no. 7.

[15] Y. Zhang, and P. Yan, "Optimal Adaptive Observer-Based Integral Sliding Mode Control of a Piezoelectric Nano-manipulator," no. February, pp. 1–8, 2017.

[16] F. Ying, C. A. Rabbath, C. Tianyou, and S. Chun-Yi, "Robust adaptive control of systems with hysteretic nonlinearities: A Duhem hysteresis modelling approach," in *AFRICON, 2009. AFRICON '09.FRICON, 2009. AFRICON '09.*, 2009, pp. 1–6.

[17] D. Habineza, M. Rakotondrabe, and Y. Le Gorrec, "Bouc-Wen Modeling and Feedforward Control of Multivariable Hysteresis in Piezoelectric Systems: Application to a 3-DoF Piezotube Scanner," *IEEE Trans. Control Syst. Technol.*, vol. 23, no. 5, pp. 1797–1806, 2015.

[18] B. Jayawardhana, R. Ouyang, and V. Andrieu, "Stability of systems with the Duhem hysteresis operator: The dissipativity approach," *Automatica*, vol. 48, no. 10, pp. 2657–2662, 2012.

[19] Q. Xu and Y. Li, "Dahl Model-Based Hysteresis Compensation and Precise Positioning Control of an XY Parallel Micromanipulator With Piezoelectric Actuation," *J. Dyn. Syst. Meas. Control*, vol. 132, no. 4, p. 41011, 2010.

[20] F. Ikhouane and J. Rodellar, "A linear controller for hysteretic systems," *IEEE Trans. Automat. Contr.*, vol. 51, no. 2, pp. 340–344, 2006.